Optic Disc Segmentation by Incorporating Blood Vessel Compensation

Ana G. Salazar-Gonzalez, Yongmin Li and Xiaohui Liu
Department of Information Systems and Computing.
Brunel University, United Kingdom

***Abstract*—Glaucoma is one of the main causes of blindness worldwide. Segmentation of vascular system and optic disc is an important step in the development of an automatic retinal screening system. In this paper we present an unsupervised method for the optic disc segmentation. The main obstruction in the optic disc segmentation process is the presence of blood vessels breaking the continuity of the object. While many other methods have addressed this problem trying to eliminate the vessels, we have incorporated the blood vessel information into our formulation. The blood vessel inside of the optic disc are used to give continuity to the object to segment.**

Our approach is based on the graph cut technique, where the graph is constructed considering the relationship between neighboring pixels and by the likelihood of them belonging to the foreground and background from prior information.

Our method was tested on two public datasets, DIARETDB1 and DRIVE. The performance of our method was measured by calculating the overlapping ratio ($Oratio$), sensitivity and the mean absolute distance (MAD) with respect to the manually labeled images. Experimental results demonstrate that our method outperforms other methods on these datasets.

***Index Terms*—Retinal images, vessel segmentation, optic disc segmentation, graph cut technique.**

I. Introduction

The morphology of the eye structures is an important indicator to evaluate the retinal health. Due to the non-invasive characteristics, image analysis is considered as the root of the research. Blood vessels can be seen as thin elongated structures in the retina, with variation in width and length, while the optic disc is the round brightest area where the blood vessels converge.

The segmentation of the blood vessels and optic disc represents the starting point of a retinal screening system. Firstly the morphology of these structures can provide information that indicates the presence of any abnormality. Furthermore the analysis can focus on the lesions (exudates and hemorrhage) once the eye structures have been identified.

The localization of the optic disc is the first step for its segmentation. Many methods for retinal image analysis have been presented in the literature. These can be classified as those that only localize the optic disc, and those that perform the segmentation as well.

Hoover et al [1] proposed a method for optic disc location based on finding the convergence of the blood vessels. In the absence of a confident convergence result the algorithm will identify the optic disc location as the brightest region in the image. In [2] the optic disc location relies on the vascular system segmentation, combining feature characteristics as retinal luminance, density, thickness and orientation of the vessels. In [3] the optic disc location is performed using a filter to match the expected directional pattern of the blood vessels. A prior vessel segmentation and a kNN regression are used to approximate the optic disc location in [4]. Kauppi et al [5] propose the use of a training stage, where PCA is adopted to determine an eigenspace that characterizes the optic disc in retinal color images. The templates are extracted from the training images and used to localize the optic disc.

The algorithms designed for the optic disc segmentation can be divided into supervised and unsupervised methods. Supervised segmentation methods can be seen as human guided classification. In [6] the location of the optic disc is performed by PCA, and a modified Active Shape Model is used to detect the disk boundary. Niemeijer et al [7] address the problem by fitting a single Point Distribution Model to the retinal images. The model contains points in the center and four extremes of the optic disc; the distances from the extremes to the center point are interpolated to find a radius **r**. A rough segmentation is marked by drawing a circle around the center point with radius **r**. The disadvantages of supervised systems are the requirement of a training process and hand labeled images, which is time and resource consuming.

Unsupervised segmentation is performed without sample classes provided by human. In [8] a multi-scale hybrid Snake is used to segment the optic disc. The method places the initial curve considering the dark area around the central bright region in Heidelberg retinal tomographs. In [9] the optic disc location is achieved using a matching template, while the segmentation is done by a deformable Contour Model. A complete automatic algorithm for the segmentation of the optic nerve is presented in [10] using scanned laser tomography images. The method is based on morphological operations, Hough transform and an anchored Active Contour Model. Walfer et al [11] present an adaptive method using mathematical morphology on fundus images.

Our purpose is to create a complete automatic and

unsupervised method capable of working on different datasets. In this paper, we present an unsupervised method for automatic optic disc segmentation using the graph cut technique. Our approach takes as a first step the localization of the optic disc based on the convergence of the blood vessels. The graph is constructed considering the relationship between neighboring pixels and the likelihood of them belonging to the foreground and background from prior information. A small sample with center in the detected optic disc area is taken as foreground seeds, while a band of pixels around the perimeter of the image are considered as background seeds. The main contribution of this paper is the use of blood vessels to provide continuity in the segmentation of the optic disc. We have introduced a compensation factor for the foreground likelihood weight using previous blood vessel segmentation.

The rest of the paper is organized as follows. In Section II we provide a brief review on graph cut technique and two different types of approximation to assign weights to the edges. The optic disc localization is described in Section III. Section IV shows our method for the optic disc segmentation including the graph construction details. Experimental results on two public datasets and performance comparison with other methods are presented in Section V.

II. Graph Cut

Graph cut is an interactive image segmentation technique in computer vision and medical image analysis [12][13][14]. The general idea is to map an image onto a graph with weighted connections. The graph is then cut (separating foreground and background), minimizing the energy function and producing the optimal segmentation for the image.

A graph $G(\nu, \epsilon)$ is defined as a set of nodes ν and edges ϵ connecting neighboring nodes. An example of graph is shown in Figure 1. There are two special nodes called terminals, *S* source (foreground) and *T* sink (background) [15]. Edges between pixels are called n-links, while t-links are referred to the edges connecting pixels to terminals. A cut is a subset of edges $C \in \epsilon$ that separates the graph into two regions, foreground and background $G(c) = \langle \nu, \epsilon \backslash C \rangle$. Each cut has a cost which is defined as the sum of the weights of the edges that it break. A globally minimum cut on a graph with two terminals can be computed efficiently in low order polynomial time via standard maxflow or push-relabel algorithms from combinatorial optimization [7].

All graph edges $e \in \epsilon$ including n-links and t-links are assigned some non negative weights. The edge weight assignment depends on different applications scenarios, but it should ensure that the energy function minimization will produce the optimal segmentation. In this paper we use two different types of approximations to assign weights to the edges: flux incorporation for blood vessel segmentation and the traditional boundary and regional terms for the optic disc.

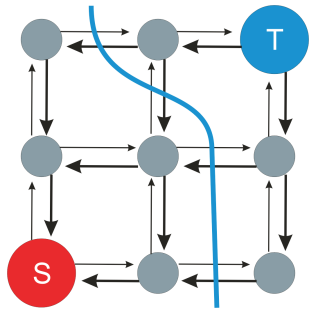

Fig. 1. Example of a graph system with terminals S (foreground) and T (background).

A. Graph for blood vessel segmentation.

The minimization of the energy function using the boundary term has a tendency to follow short edges, frequently referred to as the shrinking bias problem [16]. This problem creates particular difficulties when segmenting thin elongated structures like the blood vessels. The incorporation of flux can improve edge alignment and helps to segment thin objects such as blood vessels by keeping a balance between shrinking (length) and stretching (flux) along the boundary. The blood vessel segmentation is performed based on [17]. This approach includes the flux term into the construction of the graph designed for blood vessel segmentation.

It has been demonstrated that the flux of any given field of vector **v** can be optimized in order to improve the segmentation of elongated narrowing structures, like vessels [18] and [19]. In our implementation image gradients of the blood vessels are taken as vectors ***v***, and the flux of these vectors is incorporated into the graph and optimized.

The graph construction can be divided in two parts: the symmetric and antisymmetric parts. The symmetric part corresponds to cut geometric length and is related directly with the n-link connections. The antisymmetric part corresponds to a flux of vector field v over a cut. Specific weights for t-links are based on the decomposition of vector v. We consider a decomposition along grid edges using a natural choice of n-links oriented along the main axes.

B. Graph for optic disc segmentation

We adopt the traditional edge weight assignment presented in [15]. The energy function consists of regional and boundary terms. Regional term is calculated from the likelihood of a pixel p belonging to the foreground and background generating the t-link weights. The boundary term is based on the own pixel properties (i.e. intensity), which is used to assign weights to the n-links.

For our particular purpose we have designed a compensation factor for the foreground t-link. Details of the construction and weight assignment are presented in Section IV.

III. Optic Disc Detection

The convergence of the blood vessels is used to locate the optic disc detection. Inspired by the work presented in [11], the vessel network is segmented and the resultant binary image is pruned using a morphologic open process in order to keep the main arcade. Afterward the centroid of the arcade is located. The centroid is calculated according to:

$$C_x = \sum_{i=1}^{K} \frac{x_i}{K} \qquad C_y = \sum_{i=1}^{K} \frac{y_i}{K} \tag{1}$$

where x_i and y_i are the coordinates of the pixel in the binary image and K is the number of pixels set to "1", which is the pixels marked as blood vessels in the binary image.

Using the blue channel of the RGB retinal image, 1% of the brigthest pixels are selected. The algorithm detects the brightest area with most number of elements in the image to determine the position of the optic disc with respect to the centroid (left, right, up, down, etcetera). Considering that the main arcade is narrowing until the vessels converge, the algorithm adjusts the centroid point iteratively until it reaches the center of the arcade. The centroid point is adjusted by reducing the distance with the optic disc, and correcting its central position inside the arcade. The center of the arcade is presumed to be the vessels convergence point and the center of the optic disc. It is important to detect with accuracy the center of the optic disc, since this point will be used to automatically mark foreground seeds. A point just inside the border of the optic disc may result in some false foreground seeds. Figure 2 shows an example of optic disc center localization.

We constrain the image to a small area in order to minimize the processing time. The region of interest is constrained to a square of 200 by 200 pixels concentric with the detected optic disc center. We have selected an automatic initialization of seeds (foreground and background) for the graph. A neighborhood of 20 pixels of radius around the centre of the optic disc is marked as foreground pixels. While a band of pixels around the perimeter of the image are considered as background seeds(see Figure 3).

IV. Optic Disc Segmentation

The main difficulty in the optic disc segmentation process is the presence of blood vessels breaking the continuity of the object. Different types of approximation have attempted to solve this problem applying morphologic operation as preprocessing, in order to minimize their interference. Our approach incorporates the blood vessel information into the graph construction giving continuity to the optic disc. Prior vessel segmentation is used to perform the optic disc segmentation.

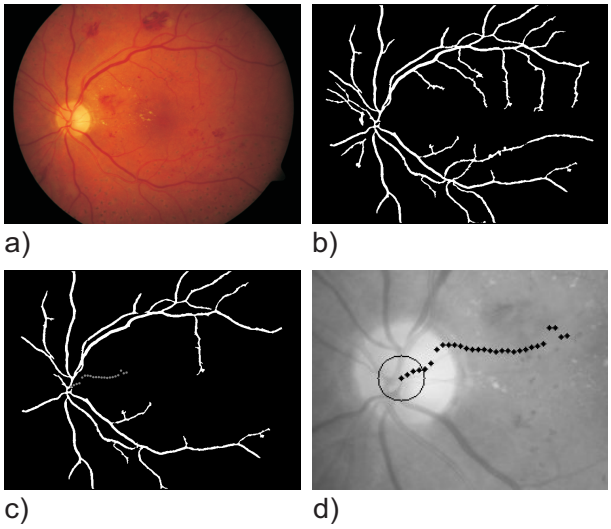

Fig. 2. Optic disc detection. a) retinal image, b) blood vessel segmentation, c) blood vessel segmentation after pruning and d) sequence of points from the centroid to the vessels convergence.

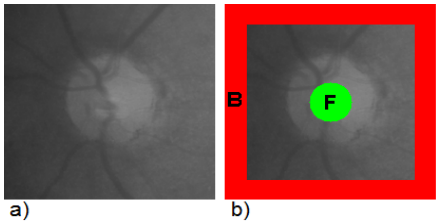

Fig. 3. a) constrained image, b) foreground **F** and background **B** seeds initialization in the constrained image.

A. Preprocessing

The original image is constrained to a region of interest concentrating the analysis in a smaller area and minimizing the processing time. The constrained image is preprocessed by applying a histogram equalization in order to enhance its contrast.

B. Graph construction

We have considered a grid of 16 pixels neighborhood. The n-link weights are defined by:

$$B_{p,q} = exp\left(-\frac{(I_p - Iq)^2}{2\sigma^2}\right) \cdot \frac{1}{dist(p,q)} \tag{2}$$

where I_p and I_q are the pixel intensities between the pixel p and its neighbor q. The distance between p and q is represented by $dist(p,q)$. Using the definition of equation (2), it is obvious that pixels with similar intensities have

strong connections. If pixels are very different, the connection between them will be very weak. The pixel links with the terminals S (foreground) and T (background) are defined by the likelihood of the pixel with the seeds. Fg_{seeds} and Bg_{seeds} are represented by the intensity distribution of the foreground and background seeds respectively. This link is calculated according to:

if $(p \neq Vessel)$

$$S_{link} = -lnPr\left(I_p|Fg_{seeds}\right)$$

$$T_{link} = -lnPr\left(I_p|Bg_{seeds}\right)$$

else

$$S_{link} = -lnPr(I_p|Fg_{seeds}) + Vad$$

$$T_{link} = -lnPr(I_p|Bg_{seeds})$$

where

$$Vad = max_{p \in Vessel}(-lnPr\left(I_p|Fg_{seeds}\right)$$

$p \neq Vessel$ implies that the pixel is not part of the vessel network. For the pixels that belong to the blood vessel network a compensation factor Vad is added for the foreground link. The dark intensity characteristic of the blood vessel pixels makes them more likely to belong to the background than the foreground. Even when vessels inside of the optic disc are less dark, the weak connection with their neighbors makes them more likely to be segmented as background.

By adding a compensation factor Vad to the foreground t-link we equilibrate this behavior. Vessels inside of the optic disc will be classified according with their neighbors connections (Foreground). Vessel pixels outside of the optic disc will have the same compensation for the foreground t-link, but because of their strong n-links to their neighbors, and those with strong t-links to the background, the segmentation will be successful.

In summary, the blood vessel classification (foreground or background) is made primarily by their neighborhood characteristics instead of their own characteristics. Finally the maxflow-v3.01 implemented by Komolgorov [1] is used in our implementation to compute the optimal segmentation.

Figure 4 shows an example of our method applied to a retinal image. The image is segmented using different values of Vad. For a low value of Vad, the segmentation is affected by the presence of the blood vessels inside or near by the optic nerve. When Vad is increased, the segmentation performance improves until it starts to segment the blood vessels as part of the foreground as well.

[1]maxflow-v3.01 is available at http://www.cs.ucl.ac.uk/staff/V.Kolmogorov/software.html.

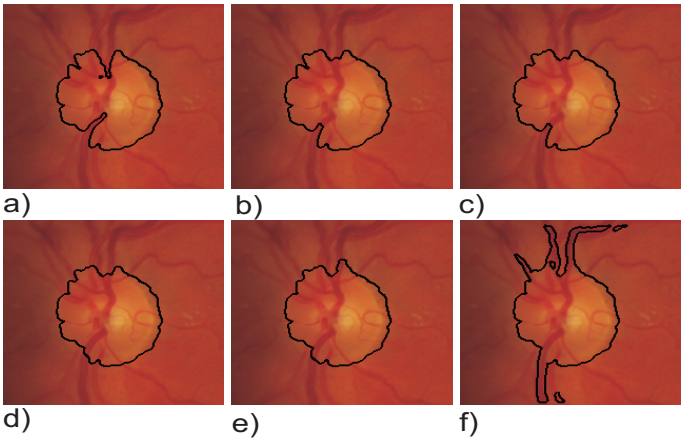

Fig. 4. Optic disc segmentation via graph cut with different foreground t-link compensation factor Vad for blood vessels: a) $Vad = 20$, b) $Vad = 50$, c) $Vad = 100$, d) $Vad = 150$, e) $Vad = 200$ and f) $Vad = 250$

V. Experiments and Results

Our proposed method was tested on two public datasets, DIARETDB1 [20] and DRIVE[21]. DIARETDB1 dataset consists of 89 images, of which 84 contain at least one sign of disease, so only 5 are considered as normal. According to [20], the data correspond to real practical situation, and images can be used to evaluate the general performance of diagnosis methods. The DRIVE dataset consists of 40 digital images, which were captured from a Canon CR5 non-mydriatic 3CCD camera at 45° field of view (FOV). The images have a size of 768×584 pixeles, eight bit per color channel.

Our algorithm detected the optic disc successful in 96.7% on the DIARETDB1 dataset and in 97.5% of the images on DRIVE. The detection of the optic disc is used to initialize foreground and background seeds.

We created hand labeled sets for DIARETDB1 and DRIVE in order to have a ground truth to compare our results. The optic disc ground truth for the DIARETDB1 and DRIVE datasets are available for research purposes at [2]. The performance of the methods was evaluated by the overlapping ratio ($Oratio$) and the mean absolute distance(MAD). The overlapping ratio is defined as:

$$Oratio = \frac{G \bigcap S}{G \bigcup S}$$

where G represents the manually segmented area and S is the area as result of the algorithm segmentation. MAD is defined as:

$$MAD(G_c, S_c) = \frac{1}{2}\left\{\frac{1}{n}\sum_{i=1}^{n} d(g_{ci}, S) + \frac{1}{m}\sum_{i=1}^{m} d(s_{ci}, G)\right\}$$

[2]http://www.brunel.ac.uk/~cspgags.

where G_c and S_c are the contour of the segmented area in the ground truth and the resulting images, and $d(a_i, B)$ is the minimum distance from the position of the pixel a_i on the contour A to the contour B. A good segmentation implies a high overlapping ratio and a low MAD value.

We calculated as well the sensitivity of the methods when they perform on DIARETDB1 and DRIVE, which is defined as:

$$Sensitivity = \frac{Tp}{Tp + Fn}$$

where Tp and Fn are the number of true positives and the number of false negatives respectively. Sensitivity is an indicator of the foreground pixels detected by the segmentation method.

Our results are compared to those provided in [11]. This method was tested on the same datasets (DIARETDB1 and DRIVE) and results were meassured under the same parameters. Also we have included the results of the traditional graph cut technique without compensation and the ones using the topology cut technique [22]. Topology cut technique introduces a label attribute for each node to handle the topology constrains, and uses a distant map to keep track of the nodes that are closest to the boundary. Unfortunately most of the methods do not present a trustworthy way to measure the results of the segmentation, making comparison of the results difficult.

Figures 5 and 6 present the segmentation results using different methods on DIARETDB1 and DRIVE datasets. The manually labeled images have been included to have a visual reference. It can be seen that our method performs better over the blood vessel interference. Particularly the traditional graph cut technique tends to segment the optic disc along the blood vessels edges. The topology cut technique succeeds in the brightest area of the optic disc where the blood vessels are more likely to look like part of the foreground. The topology cut technique was applied to the color image directly without any preprocessing. The topology cut is not an automatic technique, it requires a manual marking of foreground seeds.

Figure 7 shows the segmentation results by our method on four representative images. The images represent different challenges due to their illumination, contrast, and focal characteristics. We have included the overlapping ratio ($Oratio$) and MAD values of the segmentation result. Some authors [7] consider a minimum Oratio of 0.50 as a successful segmentation. In this direction the 100% of the images in the Figure 6 have been segmented correctly.

Figures 8 and 9 show the distribution of the overlapping ratio on DIARETDB1 and DRIVE using different segmentation methods. We have include lines as a reference at $Oratio = 50\%$ and $Oratio = 70\%$. It is obvious that our method has outperformed the traditional graph cut and the

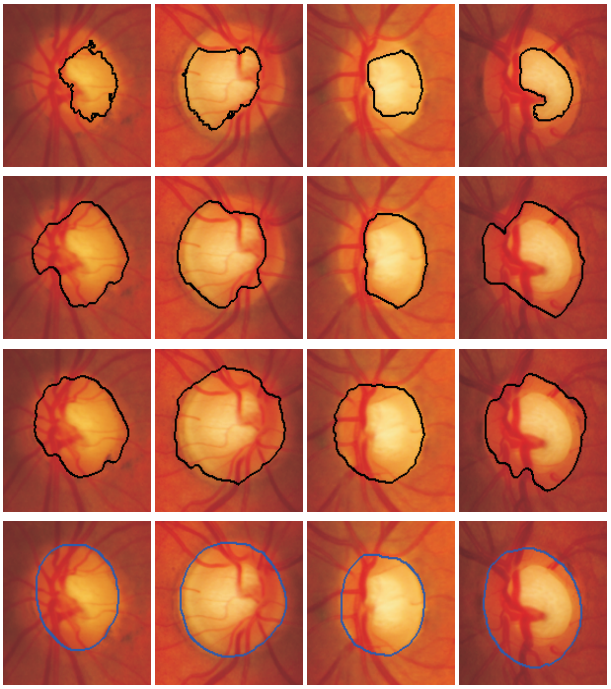

Fig. 5. Optic disc segmentation using different methods for DIARETDB1 dataset. First row: Topology cuts, second row: Graph cut, third row: Graph cut with compensation factor Vad for blood vessels and fourth row: hand labeled

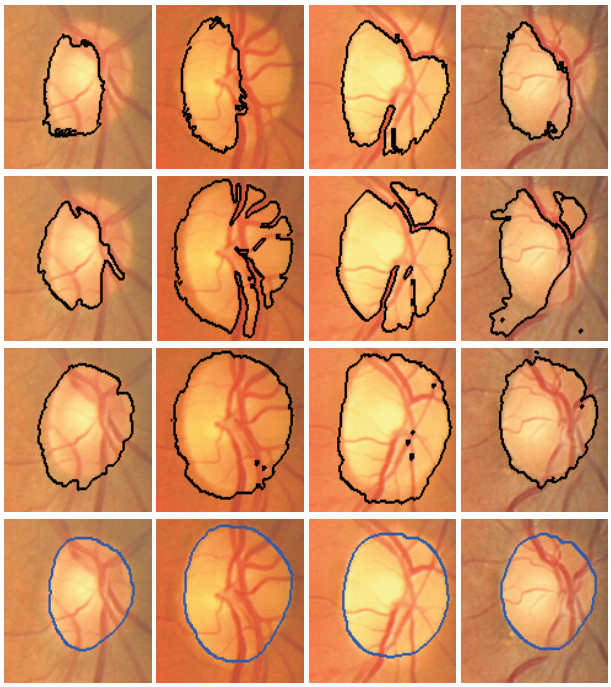

Fig. 6. Optic disc segmentation using different methods for DRIVE dataset. First row: Topology cuts, second row: Graph cut, third row: Graph cut with compensation factor Vad for blood vessels and fourth row: hand labeled

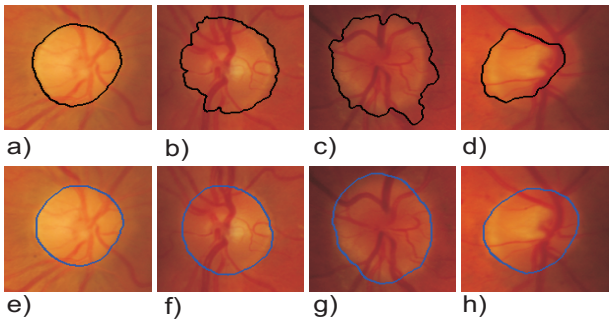

Fig. 7. Top Row: optic disc segmentation using graph cut with compensation factor Vad for blood vessels: a) Oratio = 0.9003 MAD = 2.26, b) Oratio = 0.8320 MAD = 3.94, c) Oratio = 0.7857 MAD = 5.58 and d) Oratio = 0.6393 MAD = 9.80. Bottom row: hand labeled images

topology cut techniques. It can be seen that few images were not segmented by any method due to the poor quality of the images.

Following the suggestion in [7], which takes a minimum overlapping ratio of 50% as a sucessful segmentation, we can see in the figures that the 90.6% of the images on DIARETDB1 resulted on successful segmentation using our method, and 86.5% of the images on DRIVE.

Figures 10 and 11 show the cumulative histograms comparison, for normalized overlapping ratio on DIARETDB1 and DRIVE datasets using different methods. The cumulative histogram shows the frequency of the $Oratio$ value when the segmentation is compared with the hand labelled image. In the case of a perfect matching, $Oratio = 1$, for all the images in the dataset the area under the curve would be cero. Since our method shows the minimum area under the curve, it is clear that graph cut technique using the compensation factor Vad outperforms over other techniques. The cumulative histograms provide a complete summary of the success of our method.

Table 1 and Table 2 show the comparison with different methods in terms of $Oratio$, MAD and $Sensitivity$. Our method achieved the highest overlapping ratio with the minimum MAD value. It can be seen that an increase in the overlapping ratio does not mean a decrease on MAD value necessarily. MAD value does not represent the best way to measure the segmentation results, but it provides a good reference of the contour matching with the ground truth contour reference.

VI. Conclusions

Optic disc segmentation is an important process in the analysis of retinal images. An unsupervised method based on the construction of a graph has been presented in this paper. The method incorporates the blood vessel segmentation into the graph construction, giving strength to the algorithm to

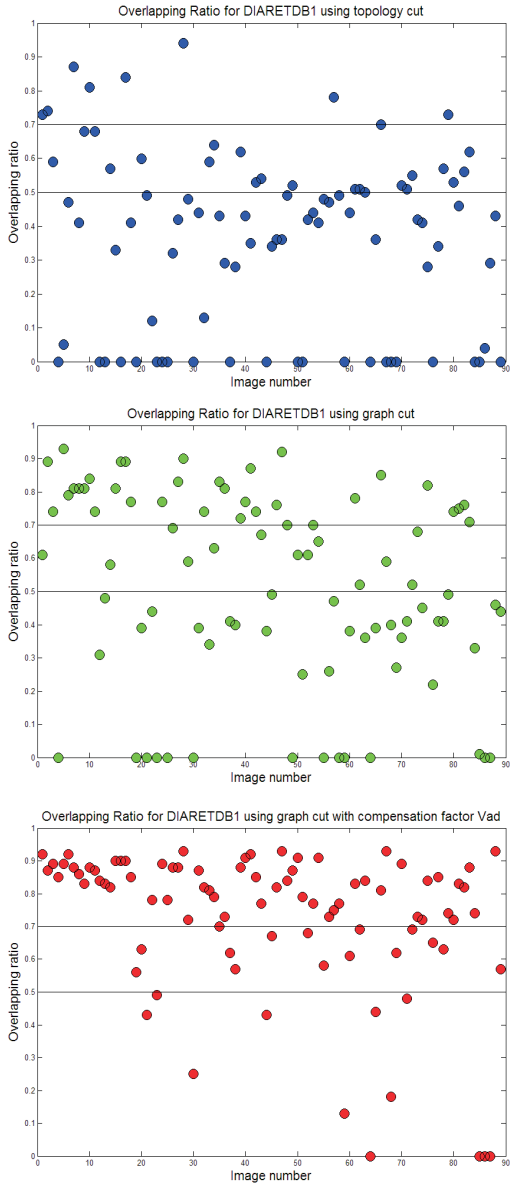

Fig. 8. Overlapping Ratio for DIARETDB1. Top: Topology cut. Centre: Graph cut. Bottom: Graph cut with compensation factor V_{ad} for blood vessels.

TABLE I
PERFORMANCE COMPARISON ON THE DIARETDB1 DATASET.

Method	Average ORatio %	Average MAD	Average Sensitivity
Topoly Cut	38.43%	17.49	55.30%
Adaptive morphologic [11]	43.65%	8.31	—
Graph Cut	54.03%	10.74	76.35%
Graph Cut with Vad	75.74%	6.38	86.55%

TABLE II
PERFORMANCE COMPARISON ON THE DRIVE DATASET.

Method	Average ORatio	Average MAD	Average Sensitivity
Topoly Cut	55.91%	10.24	65.12%
Adaptive morphologic [11]	41.47%	5.74	—
Graph Cut	55.32%	9.97	73.98%
Graph Cut with Vad	70.70%	6.68	84.44%

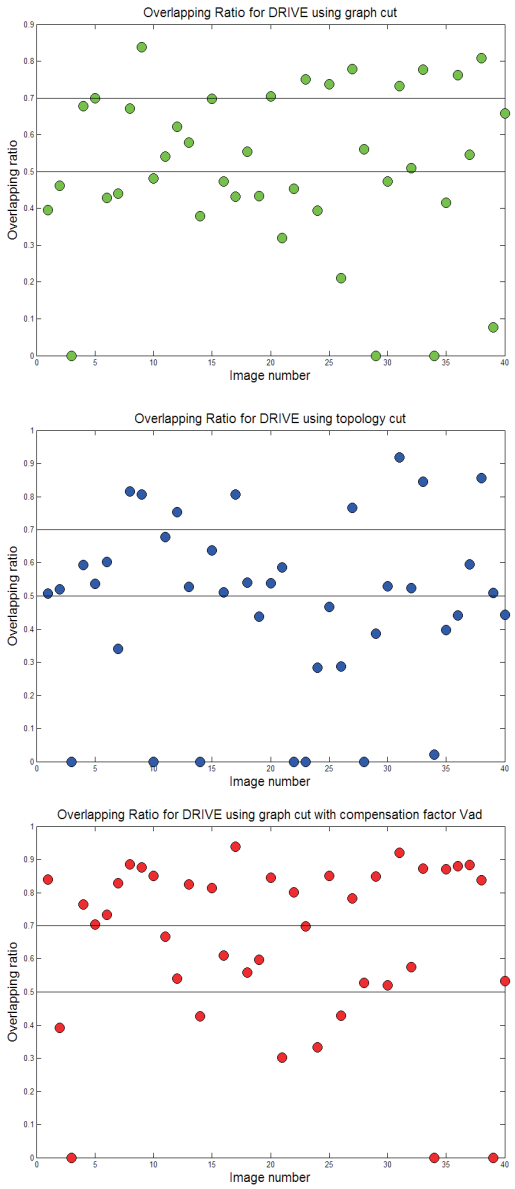

Fig. 9. Overlapping Ratio for DRIVE. Top: Topology cut. Centre: Graph cut. Bottom: Graph cut with compensation factor V_{ad} for blood vessels.

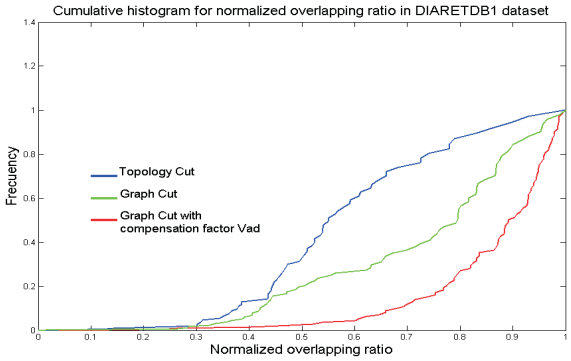

Fig. 10. Cumulative histogram for normalized overlapping ratio on DIARETDB1 dataset using different methods.

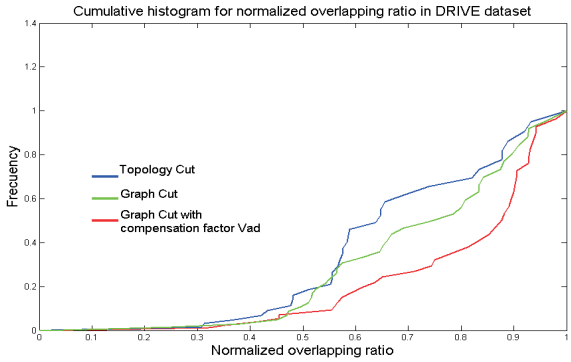

Fig. 11. Cumulative histogram for normalized overlapping ratio on DRIVE dataset using different methods.

avoid the blood vessel interference. Experimental results on DIARETDB1 and DRIVE datasets have clearly demonstrated that our method outperform other techniques such as Adaptive Morphologic [11], Topology Cut [22] and the traditional Graph Cut [15].

ACKNOWLEDGMENT

The authors would like to thank the Mexican National Council for Science and Technology (CONACYT) for financial support, and to Yun Zeng for his contribution to produce the segmentation results using the topology cut technique.

REFERENCES

[1] A. Hoover and M. Goldbaum. Locating the optic nerve in retinal image using the fuzzy convergence of the blood vessels. *IEEE Transactions on Medical Imaging*, 22(8):951–958, 2003.

[2] K. W. Tobin, E. Chaum, V. P. Govindasamy, and T. Karnowski. Detection of anatomic structures in human retinal imagery. *IEEE Transactions on Medical Imaging*, 26(12):1729–1739, 2007.

[3] A. Youssif, A. Ghalwash, and A. Ghoneim. Optic disc detection from normalized digital fundus images by means of a vessels's directed matched filter. *IEEE Transactions on Medical Imaging*, 27(1):11–18, 2008.

[4] M. Niemeijer, M. D. Abramoff, and B. van Ginneken. Automated localization of the optic disc and the fovea. *Proceedings of the 30th Annual International IEEE EMBS conference*, pages 3538–3541, 2008.

[5] T. Kauppi and H. Kalviainen. Simple and robust optic disc localisation using colour decorrelated templates. *Proceedings of advanced concepts for intelligence vision systems*, pages 719–729, 2008.

[6] H. Li and O. Chutatape. Automated feature extraction in color retinal images by a model based approach. *IEEE Transactions on biomedical engineering*, 51(2):246–254, 2004.

[7] M. Niemeijer, M. D. Abramoff, and B. van Ginneken. Segmentation of the optic disc, macula and vascular arch in fundus photographs. *IEEE Transactions on Medical Imaging*, 26(1):116–127, 2007.

[8] X. Yang, P. Morrow, and B. Scotney. Optic nerve head segmentation in hrt images. *Proceedings of the international conference on image processing*, pages 65–68, 2006.

[9] J. Lowell, A. Hunter, D. Steel, A. Basu, R. Ryder, E. Fletcher, and L. Kennedy. Optic nerve head segmentation. *IEEE Transactions on Medical Imaging*, 23(2):256–264, 2004.

[10] R. Chrastek, M. Wolf, K. Donath, H. Niemann, D. Paulus, T. Hothorn, B. Lausen, R. Lammer, C. Y. Mardin, and G. Michelson. Automated segmentation of the optic nerve head for diagnosis of glaucoma. *Medical Image Analysis*, 9(1):297–314, 2005.

[11] D. Welfer, J. Scharcanski, C. Kitamura, M. Dal Pizzol, L. Ludwig, and D. Marinho. Segmentation of the optic disc in color eye fundus images using an adaptive morphological approach. *Computers in Biology and Medicine*, 40(1):124–137, 2010.

[12] Y. Boykov and M-P. Jolly. Interactive organ segmentation using graph cuts. *In Proceedings of International Conference on Medical Image Computing and Computer-Assisted Intervention*, pages 276–286, 2000.

[13] D.R. Chittajallu, G. Brunner, U. Kurkure, R.P. Yalamanchili, and I.A. Kakadiaris. Fuzzy-cuts: A knowledge-driven graph-based method for medical image segmentation. *Proceedings of the twenty third IEEE coference on computer, vision and Pattern recognition.*, pages 715–722, 2009.

[14] J. Zhu-Jacquot and R. Zabih. Graph cuts segmentation with statistical shape prior for medical image. *Proceedings of the third international IEEE conference on signal-image technologies and internet-based system.*, pages 631–635, 2008.

[15] Y. Boykov and G. Funka-Lea. Graph cuts and efficient n-d image segmentation. *International Journal of Computer Vision*, 70(2):109–131, 2006.

[16] S. Vicente, V. Kolmogorov, and C. Rother. Graph cut based image segmentation with connectivity priors. *In Proceedings of IEEE Conference on Computer Vision and Pattern Recognition, CVPR 2008.*, 1:1–8.

[17] A. Salazar-Gonzalez, Y. Li, and X. Liu. Retinal blood vessel segmentation via graph cut. *In Proceedings of the 11th International Conference on Control, Automation, Robotics and Vision, ICARCV*, 1:225–230, 2010.

[18] A. Vasilevskiy and K. Siddiqi. Flux maximizing geometric flows. *IEEE transactions on pattern analysis and machine intelligence.*, 24(12):1565–1578, 2002.

[19] V. Kolmogorov and Y. Boykov. What metrics can be approximated by geo-cuts, or global optimization of length/area and flux. *Proceedings of the tenth IEEE international conference on computer vision*, 2005.

[20] T. Kauppi, V. Kalesnykiene, J. K. Kamarainen, L. Lensu, I. Sorri, A. Raninen, R. Voitilainen, H. Uusitalo, H. Kalviainen, and J. Pietila. Diaretdb1 diabetic retinopathy database and evaluation protocol. *In Proceedings of British Machine Vision Conference.*, 2007.

[21] J. Staal, M. D. Abramoff, M. Niemeijer, M. A. Viergever, and B. van Ginneken. Ridge-based vessel segmentation in color images of the retina. *IEEE Transactions on Medical Imaging*, 23(4):501–509, 2004.

[22] Y. Zeng, D. Samaras, W. Chen, and Q. Peng. Topology cuts: a novel min-cut/max-flow algorithm for topology preserving segmentation in n-d images. *Journal of computer vision and image understanding.*, 112(1):81–90, 2008.